Tuning excited state of bipyridyl platinum(II) complexes with bio-active flavonolate ligand: Structures, photoreactivity, and DFT calculations

Xiaozhen Han, Mehdi Sahihi, Sarah Whitfield, Ivan Jimenez

Tuning excited state of bipyridyl platinum(II) complexes with bio-active flavonolate ligand: Structures, photoreactivity, and DFT calculations

Xiaozhen Han [a], Mehdi Sahihi [b], Sarah Whitfield [a], Ivan Jimenez [a]

[a]Department of Chemistry, Stephen F. Austin State University, Nacogdoches, TX 75962, USA
[b]MSME, Univ Gustave Eiffel, UPEC, CNRS, F-77454 Marne-la-Vallée, France

Highlights

- •

  A combined experimental and theoretical study of a new series of (bpy)Pt(II) linked to a bio-active ligand.

- •

  Bipyridyl flavonolate platinum(II) complexes undergo oxygenation upon irradiation while stay stable in the dark.

- •

  The excited state of bipyridyl flavonolate platinum(II) complexes is mixed metal/ligand to ligand charge transfer (ML-LCT).

Abstract

Platinum(II) complexes with coordinated bio-active molecules that can undergo photo-induced oxygenation are finding applications in photoactivated chemotherapy (PCT). A series of bipyridyl(bpy) Pt(II) complexes with ligand flavonolate (fla^-) $[Pt^{II}BpyFla^R][BF_4]$ $[BF_4]$ (R = *p*-OMe (**1**), *p*-Me (**2**), *p*-H (**3**)) were prepared and characterized. Their photochemical and photophysical properties were investigated. Complexes **1**–**3** exhibit emission at ~530 nm, as compared to the analogous $[Pd^{II}BpyFla^R][BF_4]$ with no emission upon irradiation. In addition, Pt(II) complexes undergo oxygenation reaction with oxygen with near visible light, indicating photocleavage of ligand flavonolate. Carbon monoxide(CO) release was observed by

deoxymyoglobin from oxygenation of Pt(II) flavonolate complexes. Density functional theory calculations predict a mixed, Pt/fla- to bpy, metal/ligand-to-ligand charge transfer (ML-LCT) state in complexes **1**–**3**.

Keywords

Bipyridyl platinum (II) complexes, Flavonols, Metal/ligand-to-ligand charge transfer

1. Introduction

Since cisplatin was discovered more than six decades ago, platinum (II) complexes have attracted a lot of attention [1], [2], [3]. Cisplatin, carboplatin, and oxaliplatin (Fig. 1) are widely used anticancer drugs in clinics and proven to have high efficacy in cancer treatment, however, these compounds suffer a lack of selectivity and exhibit severe side effects [4]. The drawbacks of Pt-based anticancer drugs have motivated researchers all over the world to strive to develop new anticancer candidates with lower toxicities and higher activities toward Pt-drug resistant cancer cells [5], [6], [7], [8], [9], [10], [11], [12]. Among new approaches, photo-activated chemotherapy (PCT) is specifically relevant to our research in anticancer area. PCT is an approach where a biologically active compound is bonded to a metal center to form a complex that is nontoxic in the dark. Upon irradiation, PCT agent would release biologically active ligand as inhibitor of protein and coordinatively unsaturated metal complex which is available to bind to proteins and DNA [13], [14], [15].

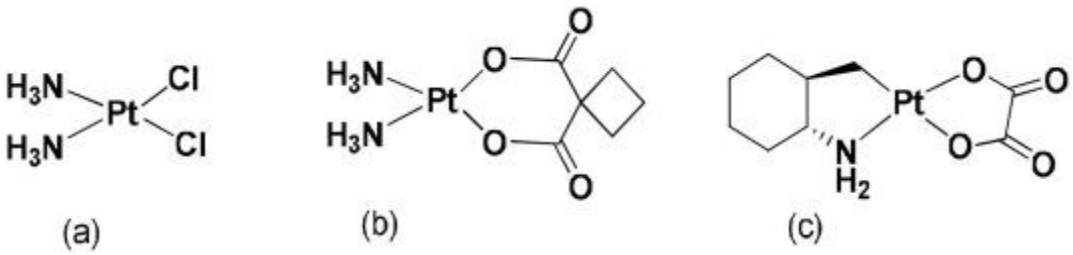

Fig. 1. Structures of (a) cisplatin, (b) carboplatin, (c) oxaliplatin.

Flavonols, naturally found in vegetables and fruits, have a wide range of biological and pharmacological activities in in-vitro studies, including anti-inflammatory, antibacterial, antiviral, antiallergic, cytotoxic, and antitumor activities [16], [17], [18], [19], [20], [21], [22], [23]. As seen in Fig. 2, a typical flavonol(3-hydroxyflavone) is composed of a benzene ring (A), condensed with a six-membered 4-pyrone ring (C) carrying a phenyl ring (B) in the 2- position and hydroxyl group in the 3-position. Flavonols can react with various divalent metals to form stable coordination compounds with bidentate binding at the hydroxyl and carbonyl groups of ring C [24], [25], [26], [27]. Our group is interested in polypridyl platinum (II) complexes because of their high performances in various photonic applications [28]. These d^8 complexes with diimine ligands are often photo-inactive in solution at room temperature due to the presence of low-lying metal centered d-d states [29]. In order to develop photo-active d^8 complexes, it is necessary to introduce strongly donating ligands to push the energy of the d-d states to higher level. Flavonolate ligands are strong π-donor ligands that serve to destabilize the HOMO and contribute to a diminished HOMO-LUMO gap. Nevertheless, there are only few d^8 metal complexes with flavonolate ligand known. In this paper, we prepared a family of photo-active complexes of $(bpy)Pt^{II}$ with biologically active ligand, 3-hydroxy flavone, and investigated their electronic and photochemical properties (Fig. 3). In addition, experimental observations were verified by DFT calculations.

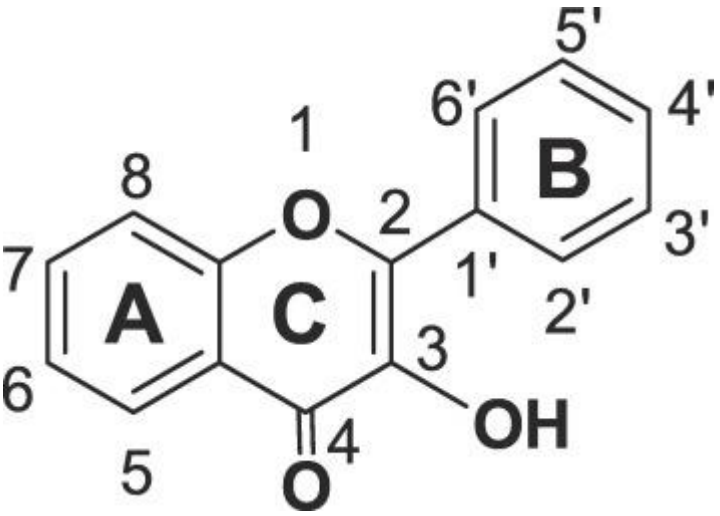

Fig. 2. Structure of 3-hydroxyflavone.

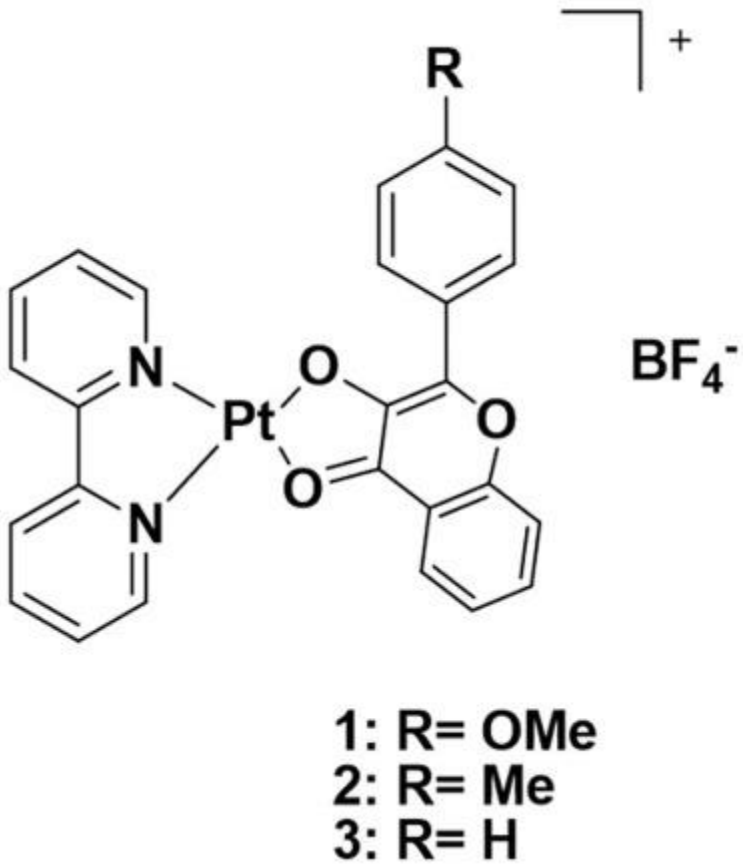

Fig. 3. Structure of bipyridyl flavonolate platinum(II) complex.

2. Experimental section

2.1. Materials and physical measurement

The reagents and solvents were obtained from commercial sources and used as received. The (2,2′-bipyridine)dichloroplatinum(II) ($Pt(Bpy)Cl_2$), silver tetrafluoroborate ($AgBF_4$), 3-hydroxyflavone (Fla), 3-hydroxy-4′-methoxyflavone (Fla-OMe), Angeli's salt, and solvents were purchased from Sigma-Aldrich. The 3-hyrdoxy-4′-methoxyflavone (Fla-Me) was obtained from Otave.

^1H NMR spectra were obtained at ambient temperature in DMSO-D^6 solution on a Jeol ECS 400 MHz NMR spectrometer. J values are given in Hz. UV–Vis spectra were recorded at ambient temperature using an Agilent HP8453 diode array spectrophotometer in a standard UV–Vis quartz cuvette. Emission and excitation spectra were recorded on a Hitachi F-4500 fluorescence spectrometer. A Rayonet Photochemical Reactor, RPR-100, equipped with RPR-5750A lamps was

used for all photochemical reactions. Accurate masses were resolved by an Accela Bundle Liquid Chromatograph (LC) coupled to a Thermo Electron Linear Trap Quadropole Orbitrap Discovery mass spectrometer. FT-IR data was collected on a Perkin Elmer Spectrum 100 FT-IR spectrometer. Elemental analyses were performed by Atlantic Microlabs Inc., Norcross, GA.

2.2. General procedure for preparation of 1–3

Silver tetrafluoroborate ($AgBF_4$) (0.4 mmol) was dissolved in methanol (4 mL); (2,2′-bipyridine) dichloroplatinum(II) ($Pt^{II}(Bpy)Cl_2$) (0.2 mmol) was dissolved in DMSO (4 mL), and then the solutions were stirred together at ambient temperature 2 h. Following gravity filtration, solid 3-hydroxyflavone derivative (0.24 mmol) and triethylamine (1 mL) were added to the filtrate. The reaction mixture was refluxed for 6 h. The corresponding platinum(II) bipyridyl flavonolate salt was then recovered using vacuum filtration and recrystallized in CH_3OH/CH_3CN solvent; remaining solvent was removed in a vacuum desiccator overnight.

[(Pt(Bpy)(3-Hydroxy-4′-methoxyfla)][BF_4]] Complex 1. Yield: 70% (green crystals) UV–Vis λ_{max} (CH_3CN/nm)($\varepsilon/M^{-1}\ cm^{-1}$) (459 (33 000); ^1H NMR (DMSO-D^6, 400 MHz): δ 8.35 (d, J = 4.5 Hz, 1H), 8.21 (d, J = 4.5 Hz, 1H), 8.06 (t, J = 16.6, 4H), 7.99 (d, J = 8.2 Hz, 2H), 7.69 (d, J = 8.5 Hz, 1H), 7.62 (t, J = 15.4 Hz, 1H), 7.48 (t, J = 12.6 Hz, 1H), 7.36 (d, J = 8.2 Hz, 2H), 7.25 (t, J = 14.9 Hz, 1H), 6.79 (d, J = 8.5 Hz, 2H) ppm, 3.83 (s, 3H) ESI-MS(+) m/z (relative intensity) calc. 618.30; found: 618.10. Elemental analysis calculated for $C_{26}H_{19}BF_4N_2O_4Pt$: C 44.28%, H 2.72%, N 3.97%. Found: C 44.21%, H 2.75%, N 3.99%.

[(Pt(Bpy)(3-Hydroxy-4′-methylfla)][BF_4]] Complex 2. Yield: 87% (green crystals) UV–Vis λ_{max} (CH_3CN/nm)($\varepsilon/M^{-1}\ cm^{-1}$) (453 (25 000); ^1H NMR (DMSO-D^6, 400 MHz): δ 8.46 (d, J = 4.8 Hz, 1H), 8.28 (d, J = 4.7 Hz, 1H), 8.16 (t, J = 5.1, 4H), 7.99 (d, J = 7.6 Hz, 2H), 7.82 (d, J = 8.1 Hz, 1H), 7.71 (t, J = 15.7 Hz, 1H), 7.54 (m, J = 17.2 Hz, 1H), 7.46 (d, J = 8.6 Hz, 1H); 7.42 (t, J = 11.3 Hz, 1H), 7.34 (t, J = 14.5, 1H), 7.10 (d, J = 7.6 Hz, 2H) ppm, 2.32 (s, 3H). ESI-MS(+) m/z (relative intensity) calc. 602.31; found: 602.10. $C_{26}H_{19}BF_4N_2O_3Pt$: C 45.30%, H 2.78%, N 4.06%. Found: C 45.33%, H 2.76%, N 4.05%.

[(Pt(Bpy)(3-Hydroxyfla)][BF_4]] Complex 3. Yield: 82% (green crystals) UV–Vis λ_{max} (CH_3CN/nm)($\varepsilon/M^{-1}\ cm^{-1}$) (449 (11 000); ^1H NMR (DMSO-D^6, 400 MHz): δ 8.81 (d, J = 5.4 Hz, 1H), 8.53 (d, J = 5.4 Hz, 1H), 8.34 (t, J = 6.8, 4H), 8.25 (m, J = 7.2 Hz, 2H), 8.11 (d, J = 4.1 Hz, 1H), 7.84 (t, J = 7.8 Hz, 1H), 7.73 (d, J = 4.5 Hz, 1H), 7.67 (t, J = 6.5 Hz, 1H), 7.51

(m, 5H). ESI-MS(+) *m/z* (relative intensity) calc. 588.29; found: 588.10. $C_{25}H_{17}BF_4N_2O_3Pt$: C 44.47%, H 2.54%, N 4.15%. Found: C 44.48%, H 2.50%, N 4.14%.

2.3. Oxygenation reaction of 1–3 with O_2 upon irradiation

A stock solution (1 mM, 50 µL) of **1** in DMSO in an argon atmosphere was added to oxygen saturated acetonitrile (2 mL) in a screw-capped UV cuvette. The cuvette was irradiated with light $\lambda_{irr} \geq 360$ nm by bandpass (Thorlabs) filters then monitored by UV–Vis spectroscopic analysis in 10 min. intervals for a total of 80 min. The experiment was repeated with complexes **2** and **3**.

2.4. CO trapping by deoxymyoglobin

The oxygenated product of complex **1** was prepared following the literature [27a]. Complex **1** (20 mg) was put in a one – neck flask with 20 mL acetonitrile. Bubble oxygen into flask for 7 mins. The flask was taken to Xe lamp with a filter (only pass ≥ 360 nm) in front of lamp and stirred under O_2 for 20 mins. The oxygenated complex **1** was collected by evaporating solvent under vacuum.

CO trapping was carried out in a long-necked quartz cuvette attached via side arm to a 10 mL round bottom flask. A 6.2 µM sample of deoxymyoglobin in 3 mL pH 7.0 phosphate buffer was added to the cuvette; a 2 mM of solution of oxygenated complex **1** in MeCN was added to the round-bottom flask and the reaction was initiated by Xe lamp. The generation of CO-Fe^{II}Mb, via diffusion of CO through the side arm, was observed by a shift of the Soret absorbance peak from 434 to 423 nm.

2.5. Computational procedure

All QM calculations were performed by Gaussian09 package [30] using DFT and TD-DFT for the electronic ground states (GSs) and excited states (ESs), respectively. CAM-B3LYP [31] functional and LANL2DZ [32] basis set were used to optimize ground and excited state geometries as well as to determine the absorption spectrum. In all TD-DFT calculations, the first sixty singlet ESs were considered to study the absorption. Calculations were done in acetonitrile with implicit solvation using the polarizable continuum model (PCM) [33]. Molecular orbitals (MOs) from the Gaussian calculations were plotted using the VMD [34] program. The analysis of the MO compositions was performed using the GaussSum program [35].

3. Results and discussion

3.1. Synthesis and characterization

To synthesize the bipyridyl flavonolate Pt(II) complexes [$Pt^{II}BpyFla^{R}$][BF_4](R = *p*- OMe (**1**), *p*-Me (**2**), *p*-H **3**)**),** (2,2′-bipyridine)dichloroplatinum(II) (1.0 eq) dissolved in DMSO was mixed with silver tetrafluoroborate (2.0 eq) dissolved in methanol to precipitate AgCl and generate [$Pd^{II}Bpy(sol)_2$] moiety. After filtration, solid 3-hydroxyflavone derivative (1.2 eq) was added to the filtrate, along with triethylamine to deprotonate flavonols. After 6 h refluxing, the products were recovered, recrystallized in CH_3OH/CH_3CN solvent, and dried under vacuum. All complexes **1**–**3** are relatively stable under air in solid state. The complexes have been characterized by ^{1}H NMR spectroscopy, positive mode electrospray ionization mass spectrometry (ESI-MS +), UV–Vis and infrared spectroscopies, and elemental analysis. In general, the ^{1}HNMR spectra of **1**–**3** in DMSO-d_6 exhibit bipyridyl resonances in the 8.0 – 9.0 ppm range that are typical for protons in bipyridyl compounds and ligand flavonolate resonances in the 6.8–7.8 ppm range (Figs. S1–S3). The peak assigned to the methoxy group in complex **1** is seen at 3.8 ppm. The peak assigned to the methyl group in complex **2** is seen at 2.3 ppm. Each complex in ESI-MS(+) shows one peak cluster that can be assigned to [$Pt^{II}BpyFla^{R}$]$^+$ (*m*/*z* (pos.) = 618.10 for **1**, 602.10 for **2**, and 588.09 for **3**). The *m*/*z* value and isotope distribution pattern of each peak cluster match well with the calculated value (Figs. S4–S6), indicating that each complex keeps its oxidation state and mononuclear structure in solution.

3.2. Spectroscopic properties of the complexes 1–3

Bipyridyl flavonolate Pt(II) complexes (**1**–**3**) have very similar IR and electronic spectra (Table 1). FT-IR spectra shows the presence of functional group of carbonyl (-C O). Shifts in their characteristic absorbance peaks help determine how ligands are coordinated with the metal. The C O stretching vibration of the coordinated carbonyl in the ligand of complexes **1**–**3** are between 1450 and 1500 cm^{-1}, shifted to 102–152 cm^{-1} lower energies compared to the free 3-hydroxyflavone (1602 cm^{-1}) [24], [25], [26]. This shift of lower energies can be explained by the formation of a five-membered chelate ring as the metal bonds to the carbonyl oxygen of the flavonolate ligand [24], [25], [26], [27].

Table 1. Summary of FT-IR ,UV–Vis absorption, and emission data for Pt(II) bipyridyl flavonolate complexes.

Complex	λ_{max} (nm)	Ext. Coeff. (M^{-1} cm^{-1})	ν_{CO} (cm^{-1})	Ex. λ_{max} (nm)	Em. λ_{max} (nm)	σ[a]
1	459	3.3x 10^4	1450	364	535	−0.27
2	453	2.5x 10^4	1460	358	532	−0.17
3	449	1.1x 10^4	1500	344	532	0

a

Hammett constants σ for substituents (OCH_3, CH_3, and H)[5].

When dissolved in DMSO under anaerobic conditions, each complex **1**–**3** (Fig. 4a) exhibits an electronic absorption maxima between 449 and 459 nm (complex **1**: 459 nm ($\varepsilon = 3.3 \times 10^4$ $M^{-1}cm^{-1}$), complex **2**: 453 nm ($\varepsilon = 2.5 \times 10^4$ $M^{-1}cm^{-1}$), complex **3**: 449 nm ($\varepsilon = 1.1 \times 10^4$ $M^{-1}cm^{-1}$)), assigned to the π-π* transition as is typical in metal flavonolate complexes. The λ_{max} of Pt(II) bipyridyl flavonolate complexes $[Pt^{II}BpyFla^{R}]BF_4$ are red-shifted around 15 nm as compared to similar $[Pd^{II}BpyFla^{R}]BF_4$ [27]. $[Pt^{II}BpyFla]^+$ is blue-shifted about 10 nm relative to those of free flavonolate (458 nm for Me_4NFla [24] and 465 nm for KFla [36], [37]). Furthermore, the λ_{max} values of the complexes are in order of **1** > **2** > **3**, and the plot of the λ_{max} vs Hammett constant σ is linear (R = 0.93) [38]. The largest λ_{max} was observed in complex **1**, bearing the strongest electron-donating group (OMe), presumably due to the best planarity and conjugation in flavonolate molecule of **1**, as confirmed by its smallest torsion angle in $[Co^{II}L^{R}Fla]$ complexes [24], [25]. These results indicate that the λ_{max} of the coordinated

flavonolate is also affected by the electronic nature of the substituent group in the ligands.

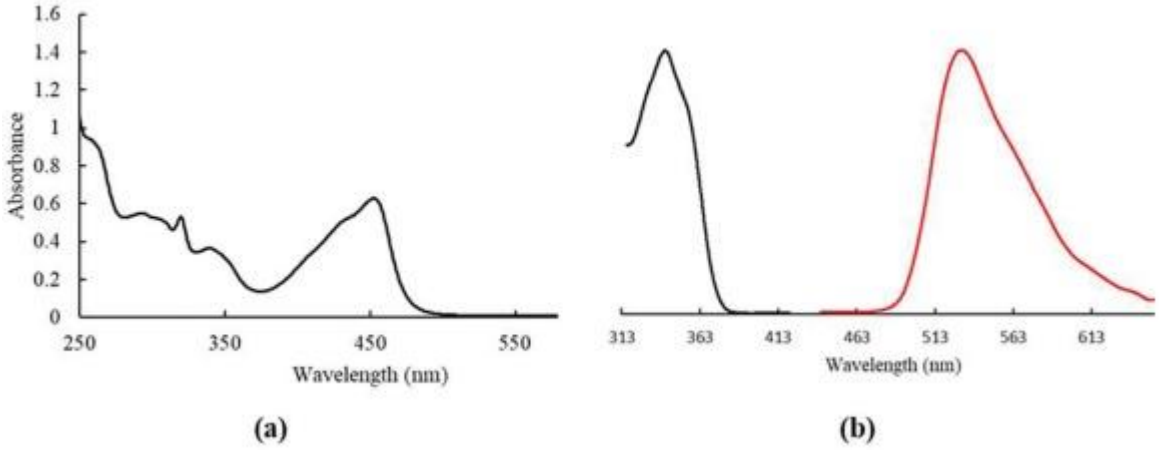

Fig. 4. (a) UV–Vis spectrum of complex **3** (25 μM in acetonitrile); (b) Action spectra of complex **3** in acetonitrile at room temperature.

The action spectra of complex **3** in acetonitrile at room temperature is shown in Fig. 4b; excitation of a transition centered at 350 nm, attributable to the flavonolate, elicits an emission at 532 nm. This behavior strongly resembles that described for Cd^{2+} and Hg^{2+} flavonolate complexes which also undergo photo-induced dioxygenation and photo-cleavage of ligand flavonolate [24], [25], [26]. This excitation is critical to the reaction with O_2 as no oxygenation was observed in analogous $[PdBpyFla^{R}]^{+}$ complexes due to the lack of photosensitivity [27c].

3.3. Electronic structure calculations

To gain further insight into the electronic structures of **1**–**3**, these complexes were investigated by means of DFT and TD-DFT methods. A preliminary study of the calculated electron properties of **3** was performed to assess the validity of the adopted theoretical modeling for the investigated compounds by comparison with the experimental results presented. The calculated molecular orbitals (MOs) and Mulliken population densities for **1** are shown in Fig. 5 (Figs. S7–S8 for **2** and **3**) and Table 2 (Table S1 for **2** and **3**).

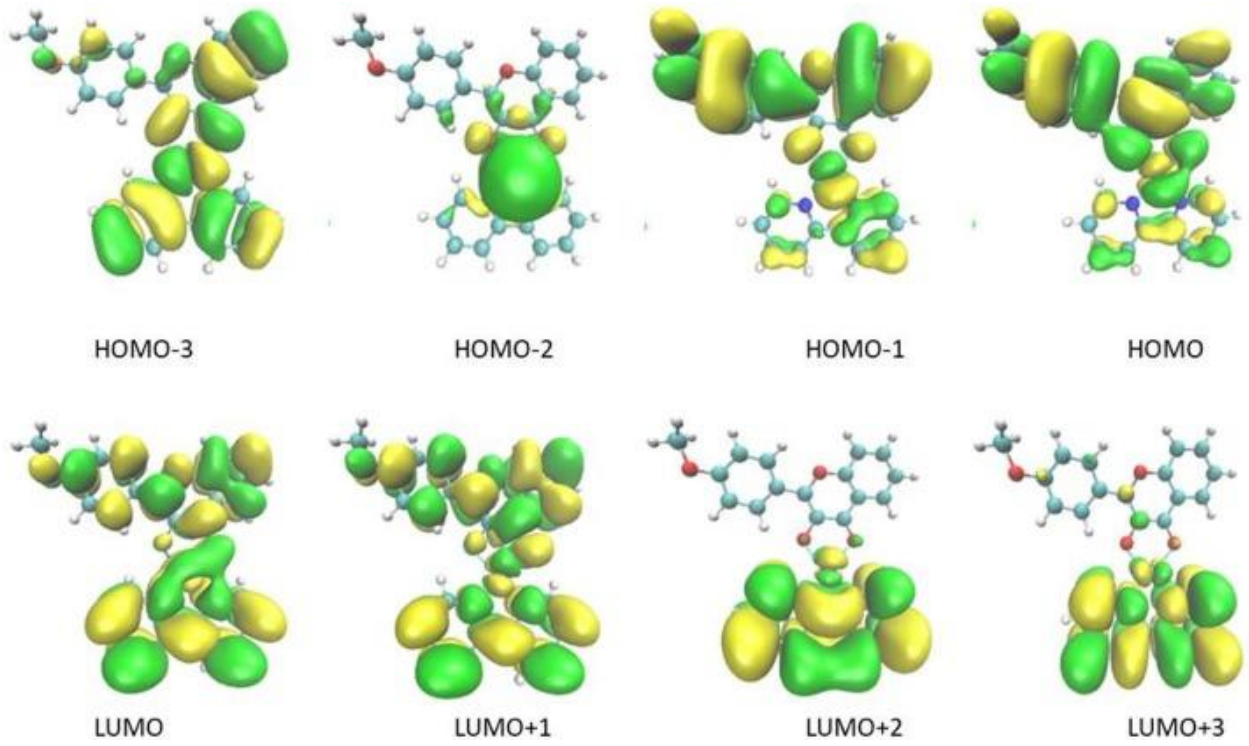

Fig. 5. Calculated frontier molecular orbitals for complex **1**.

Table 2. Percent contribution of selected MOs and corresponding energies (E_{MO}) of complex **1.**

MO	**Complex 1**			
	% Contribution			**E_{MO} (eV)**
	Pt	**Bpy**	**Fla-OMe**	
LUMO + 3	1	98	1	−1.85
LUMO + 2	1	98	1	−1.95
LUMO + 1	3	61	36	−2.87
LUMO	3	58	39	−3.06
HOMO	10	3	87	−5.91
HOMO-1	13	3	84	−6.84

MO	Complex 1			
	% Contribution			E_{MO} (eV)
	Pt	Bpy	Fla-OMe	
HOMO-2	91	3	7	−7.00

As displayed in Fig. 5 and Table 2, HOMO of complex **1** in the ground state is mainly flavonolate ligand (Fla-OMe) (87%) with minor contributions from Pt (10%) and bipyridine (bpy) (3%) while the LUMO is of mixed bpy (58%) and Fla-OMe (39%). The calculated data evidence that the flavonolate ligand characterizes the high occupied MOs (HOMO and HOMO-1), while the bpy ligand occupies the low virtual ones (LUMO, LUMO + 1, and LUMO + 2), in agreement with what was established by previous investigation on this class of complexes [39]. A significant contribution by the d orbitals of Pt(II) only occurs in the inner occupied MOs where the dz^2 orbital describes the HOMO-2. The calculated MOs and Mulliken population densities of **2** and **3** show similar properties to **1**. The calculated electronic absorption spectra of **1**–**3** using TD-DFT are in good agreement with experimental data. The energy transition in **1** is predicted to be a metal/ligand-to-ligand charge transfer (ML-LCT) from HOMO (Pt/fla^-) to LUMO (bpy) with a maximum at 510 nm, corresponding to the experimentally observed absorption feature at 459 nm. The slightly higher-energy shoulder transition at 440 nm is calculated at 461 nm from HOMO (Pt/fla^-) to LUMO + 1 (bpy) (Figs. S9–S11, Tables S2–S4).

The charge distribution among fla^-, bpy, and Pt(II), obtained as a sum of natural charges calculated through the natural bond order (NBO) analysis [40] displays that the electron density is polarized toward the flavonolate ligand (Table 3). Moreover, the formally divalent Pt compensates its lack of electron through its bonds with two ligands. In fact, Pt acts both as an electron donor toward the Rydberg orbitals of the two ligands and as an electron acceptor from the occupied orbitals of the O and O atoms through its 5d6s atomic orbitals [41].

Table 3. Comparison among the NBO partial charges over the fragments.

Complex	NBO charge		
	Pt(II)	Bpy	Fla
1	0.754	0.580	−0.334
2	0.756	0.585	−0.341
3	0.758	0.588	−0.346

3.4. Photo-induced oxygenation of complexes 1–3 with O_2

The photo-induced oxygenation reaction of complexes **1** was monitored through changes in the electronic absorbance at λ_{max} in acetonitrile at room temperature as a function of irradiation time (Fig. 6). The irradiation of oxygen-purged sample of **1** results in a decrease in MLCT band at 459 nm as a function of irradiation time with $\lambda_{irr} \geq 360$ nm. During the photolysis of **1**, the MLCT band disappear gradually, indicating the cleavage of ligand flavonolate. Similar results were observed for **2** and **3**. It should also be noted that no changes to the electronic absorption spectra of **1**–**3** were observed in the absence of light for at least 48 h in acetonitrile and H_2O (5% DMSO), consistent with the dark stability of the complexes. Using deoxygmyoglobin as a trap, we also confirm that oxygenation of **1** leads to CO release [27]. Fig. 7 displays the UV–Vis spectra of deoxymyoglobin and CO-myoglobin. The progress of the reaction was monitored by the shift in Soret absorbance from 434 to 423 nm, confirming formation of CO-Fe^{II}Mb.

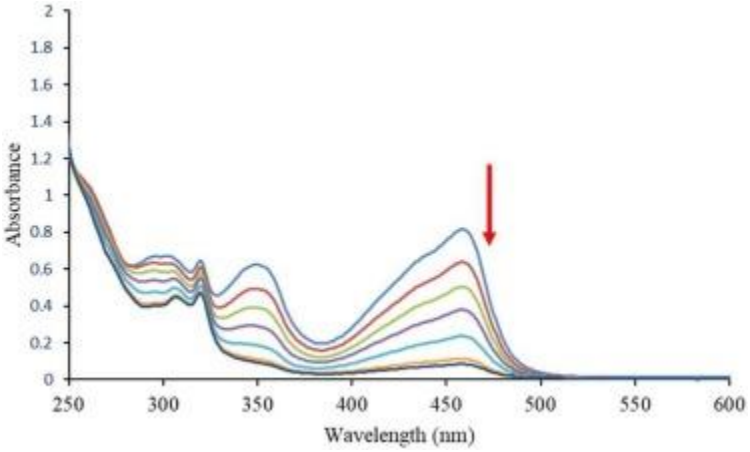

Fig. 6. UV–Vis absorption spectra change of the reaction of complex **1** with O_2 upon irradiation.

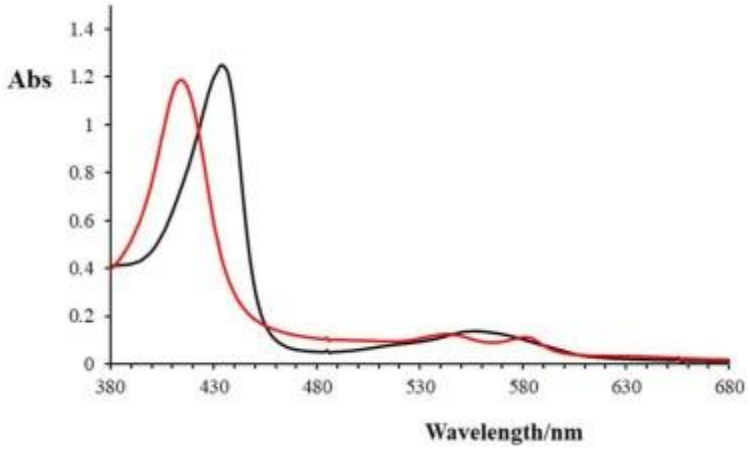

Fig. 7. UV–Vis spectra of formation of CO-Fe^{II}Mb (red line) by trapping of CO by deoxy-myoglobin (black line) released in the reaction of complex **1** with oxygen. (For interpretation of the references to colour in this figure legend, the reader is referred to the web version of this article.)

It is important to note that the bipyridyl flavonolate Pt(II) complexes **1**–**3** possess the HOMO with significant contribution from the flavonolate ligand, indicating that the fla- ligand is easily oxidized by O_2 through the likely pathway of photoinduced electron transfer to O_2. Similar mechanism was proposed in the analogous system of bis-bipyridyl flavonolate ruthenium (II) complexes with O_2 upon light irradiation [27]. More information on the mechanism is a topic of future work.

4. Conclusions

In summary, three bipyridyl flavonolate Pt^{II} complexes were synthesized and characterized by UV–Vis, ^{1}H NMR, FTIR, ESI-MS(+) and elemental analysis. The electronic structure and electronic absorption properties were investigated by DFT and TD-DFT calculations, the results of which indicate metal/ligand-to-ligand charge transfer (ML-LCT) in the excited state of bipyridyl flavonolate Pt(II) complexes. The photo-induced reaction of **1**–**3** with dioxygen was observed. These complexes are stable in the dark but undergo oxygenation reaction upon irradiation to cleave ligand flavonolate. Future work will focus on mechanism of photo-induced oxygenation.

5. Associated content

The supporting information is available on the Web site. Data include ESI-MS(+), NMR, UV–Vis and DFT, TD-DFT calculations.

CRediT authorship contribution statement

Xiaozhen Han: Conceptualization, Methodology, Validation, Formal analysis, Writing - original draft, Writing - review & editing, Supervision. **Mehdi Sahihi:** Methodology, Data curation, Visualization. **Sarah Whitfield:** Investigation, Visualization. **Ivan Jimenez:** Investigation, Visualization.

Declaration of Competing Interest

The authors declare that they have no known competing financial interests or personal relationships that could have appeared to influence the work reported in this paper.

Acknowledgment

We greatly thank Dr. Christopher Becker and Dr. Alejandro Ramirez from Mass Spectrometry Center, Baylor University, for the help in high-resolution mass spectrometry. We gratefully acknowledge the financial support of the Welch Foundation Grant (AN-0008), the Texas Academy of Science and Faculty Research/ Creative Activity Grant (150030-26212-150) from Stephen F. Austin State University.

References

[1] B. Rosenberg, L. Van Camp, T. Krigas, Nature 205 (4972) (1965) 698–699.

[2] P.M. Takahara, A.C. Rosenzweig, C.A. Frederick, S.J. Lippard, Nature 377 (6550) (1995) 649–652.

[3] T.C. Johnstone, K. Suntharalingam, S.J. Lippard, Chem. Rev. 116 (5) (2016) 3436–3486.

[4] L. Kelland, Nat. Rev. Cancer 7 (8) (2007) 573–584.

[5] R.G. Kenny, C.J. Marmion, Chem. Rev. 119 (2) (2019) 1058–1137.

[6] L. Zeng, P. Gupta, Y. Chen, E. Wang, L. Ji, H. Chao, Z.-S. Chen, Chem. Soc. Rev. 46 (19) (2017) 5771–5804.

[7] R. Trondl, P. Heffeter, C.R. Kowol, M.A. Jakupec, W. Berger, B.K. Keppler, Chem. Sci. 5 (8) (2014) 2925–2932.

[8] A. Notaro, G. Gasser, Chem. Soc. Rev. 46 (23) (2017) 7317–7337.

[9] S. Saha, B. Peña, K.R. Dunbar, Inorg. Chem. 58 (21) (2019) 14568–14576.

[10] T.N. Rohrabaugh, K.A. Collins, C. Xue, J.K. White, J.J. Kodanko, C. Turro, Dalt. Trans. 47 (34) (2018) 11851–11858.

[11] M.H. Al-Afyouni, T.N. Rohrabaugh, K.F. Al-Afyouni, C. Turro, Chem. Sci. 9 (32) (2018) 6711–6720.

[12] D. Havrylyuk, K. Stevens, S. Parkin, E.C. Glazer, Inorg. Chem. 59 (2) (2020) 1006–1013.

[13] S. Bonnet, Dalt. Trans. 47 (31) (2018) 10330–10343.

[14] A.D. Ostrowski, P.C. Ford, Dalt. Trans. 48 (2009) 10660–10669.

[15] J.D. Knoll, B.A. Albani, C. Turro, Acc. Chem. Res. 48 (8) (2015) 2280–2287.

[16] C. Guohua, S. Emin, L. Ronald, Free Radical Biol. Med. 22 (1997) 749–760.

[17] L. Van Hoof, D.A. Van den Berghe, G.M. Hatfield, A.J. Vlietinck, Planta Med. 50 (1984) 513–517.

[18] T. Brasseur, J. Pharm. Belg. 44 (1989) 235–241.

[19] B.L. Wei, C.M. Lu, L.T. Tsao, J.P. Wang, C.N. Lin, Planta Med. 67 (2001) 745–747.

[20] M. Fischer, G.D. Mills, T.J. Slaga, Carcinogenesis 3 (1982) 1243–1245.

[21] M. Huang, T. Ferraro, in: M.T. Huang, C.T. Ho, C.Y. Lee (Eds.), Phenolic Compounds in Food and their Effect on Health II, ACS Symposium Series; American Chemical Society, Washington, DC, 1992, Chapter 2, p. 507.

[22] M.T. Huang, A.W. Wood, H.L. Newmark, J.M. Sayer, H. Yagi, D.M. Jerina, A.H. Conney, Carcinogenesis 4 (1983) 1631–1637.

[23] M. Musialik, R. Kuzmicz, G. Litwinienko, J. Org. Chem. 74 (2009) 2699–2709.

[24] (a) J. Kaizer, G. Barath, J.S. Pap, G. Speier, Chem. Commun. (2007) 5235–5237; (b) A. Matuz, M. Giorgi, G. Speier, J. Kaizer, Polyhedron 63 (2013) 41–49; (c) É. Balogh-Hergovich, J. Kaizer, G. Speier, V. Fulop, L. Parkanyi, Inorg. Chem. 38 (1999) 3787–3795; (d) L. Barhacs, J. Kaizer, G.J. Speier, Mol. Catal. A. 172 (2001) 117–125; (e) J. Kaizer, J. Pap, G. Speier, L. Párkányi, Eur. J. Inorg. Chem. (2004) 2253–2259; (f) É. Balogh-Hergovich, J. Kaizer, J. Pap, G. Speier, G. Huttner, L. Zsolnai, Eur. J. Inorg. Chem. (2002) 2287–2295.

[25] (a) K. Grubel, K. Rudzka, A.M. Arif, K.L. Klotz, J.A. Halfen, L.M. Berreau, Inorg. Chem. 49 (2010) 82–96; (b) K. Grubel, B.J. Laughlin, T.R. Maltais, R.C. Smith, A.M. Arif, L.M. Berreau, Chem. Commun. 47 (2011) 10431–10433.

[26] (a) Y.J. Sun, Q.Q. Huang, J.J. Zhang, Inorg. Chem. 53 (2014) 2932–2942; (b) Y.J. Sun, Q.Q. Huang, T. Tano, S. Itoh, Inorg. Chem. 52 (2013) 10936–10948.

[27] (a) X. Han, M.R. Kumar, A. Hoogerbrugge, K.K. Klausmeyer, M.M. Ghimire, L.M. Harris, M.A. Omary, P.J. Farmer, Inorg. Chem. 57 (2018) 2416–2424; (b) X. Han, K.K. Klausmeyer, P.J. Farmer, Inorg. Chem. 55 (15) (2016) 7320–7322; (c) X. Han, S. Whitfield, J. Cotten, Transit. Met. Chem. 45 (2020) 217–225.

[28] M. Hissler, J.E. McGarrah, W.B. Connick, D.K. Geiger, S.D. Cummings, R. Eisenberg, Coord. Chem. Rev. 208 (2000) 115–137.

[29] J.A. Weinstein, M.T. Tierney, E.S. Davies, K. Base, A.A. Robeiro, M.W. Grinstaff, Inorg. Chem. 45 (2006) 4544–4555.

[30] M.J. Frisch, G.W. Trucks, H.B. Schlegel, G.E. Scuseria, M.A. Robb, J.R. Cheeseman, G. Scalmani, V. Barone, B. Mennucci, G.A. Petersson, H. Nakatsuji, M. Caricato, X. Li, H.P. Hratchian, A.F. Izmaylov, J. Bloino, G. Zheng, J.L. Sonnenberg, M. Hada, M. Ehara, K. Toyota, R. Fukuda, J. Hasegawa, M. Ishida, T. Nakajima, Y. Honda, O. Kitao, H. Nakai, T. Vreven, J.A. Montgomery, J.E. Peralta Jr., F. Ogliaro, M. Bearpark, J.J. Heyd, E. Brothers, K.N. Kudin, V.N. Staroverov, R. Kobayashi, J. Normand, K. Raghavachari, A. Rendell, J.C. Burant, S.S. Iyengar, J.

Tomasi, M. Cossi, N. Rega, J.M. Millam, M. Klene, J.E. Knox, J.B. Cross, V. Bakken, C. Adamo, J. Jaramillo, R. Gomperts, R.E. Stratmann, O. Yazyev, A.J. Austin, R. Cammi, C. Pomelli, J.W. Ochterski, R.L. Martin, K. Morokuma, V.G. Zakrzewski, G.A. Voth, P. Salvador, J.J. Dannenberg, S. Dapprich, A.D. Daniels, O. Farkas, J.B. Foresman, J.V. Ortiz, J. Cioslowski, D.J. Fox, GAUSSIAN 09, Revision A. 02, Gaussian, Inc., Wallingford, CT, 2009.

[31] T. Yanai, D.P. Tew, N.C. Handy, Chem. Phys. Lett. 393 (2004) 51–57.

[32] P.J. Hay, W.R. Wadt, J. Chem. Phys. 82 (1985) 270. J. C4.4.hem. Phys. 82 (1985) 284.

[33] S. Miertuˇs, E. Scrocco, J. Tomasi, Chem. Phys. 55 (1981) 117–129.

[34] W. Humphrey, A. Dalke, K.J. Schulten, Mol. Graphics 14 (1996) 33–38.

[35] N.M. O'Boyle, A.L. Tenderholt, K.M. Langner, J. Comp. Chem. 29 (2008) 839–845.

[36] L. Barhács, J. Kaizer, G. Speier, J. Org. Chem. 65 (2000) 3449–3452.

[37] J.S. Pap, A. Matuz, G. Baráth, B. Kripli, M. Giorgi, G. Speier, J. Kaizer, J. Inorg. Biochem. 108 (2012) 15–21.

[38] D.H. McDaniel, H.C. Brown, J. Org. Chem. 23 (1958) 420–427.

[39] (a) J. Best, I.V. Sazanovich, H. Adams, R.D. Bennett, E.S. Davies, A. Meijer, M. Towrie, S.A. Tikhomirov, O.V. Bouganov, M.D. Ward, J.A. Weinstein, Inorg. Chem. 49 (2010) 10041–10056; (b) N.M. Shavaleev, E.S. Davies, H. Adams, J. Best, J.A. Weinstein, Inorg. Chem. 47 (2008) 1532–1547.

[40] (a) J.P. Foster, F. Weinhold, J. Am. Chem. Soc. 102 (1980) 7211–7218; (b) A.E. Reed, L.A. Curtiss, F. Weinhold, Chem. Rev. 88 (1988) 899–926; (c) A.E. Reed, R.B. Weinstock, F. Weinhold, J. Chem. Phys. 83 (1985) 735–746.

[41] J. Moussa, L.M. Chamoreau, A. Degli Esposti, M.P. Gullo, A. Barbieri, H. Amouri, Inorg. Chem. 53 (13) (2014) 6624–6633.